

originally published as:

Maus, S., McLean, S., Dater, D., Lühr, H., Rother, M., Mai, W., Choi, S. (2005): NGDC/GFZ candidate models for the 10th generation International Geomagnetic Reference Field. – EARTH PLANETS SPACE, 57, 12, 1151-1156.

NGDC/GFZ candidate models for the 10th generation International Geomagnetic Reference Field

Stefan Maus^{1,2}, Susan McLean¹, David Dater¹, Hermann Lühr³, Martin Rother³, Wolfgang Mai³, and Sungchan Choi³

¹National Geophysical Data Center, NOAA E/GC1, 325 Broadway, Boulder, CO 80305, USA

²Cooperative Research Institute for Research in Environmental Sciences, University of Colorado, USA

³GeoForschungsZentrum, 14473 Potsdam, Germany

(Received February 9, 2005; Revised July 5, 2005; Accepted July 5, 2005)

Following the call for candidates for the 10th generation IGRF, we produced and submitted three main field and three secular variation candidate models. The candidates are derived from parent models which use a standard quadratic parameterisation in time of the internal Gauss coefficients. External magnetospheric fields are represented by combined parameterisations in Solar Magnetic (SM) and in Geocentric Solar Magnetospheric (GSM) coordinates. Apart from the daily and annual variations caused by these external fields, the model also accounts for induction by Earth rotation in a non-axial external field. The uncertainties of our candidates are estimated by comparing independent models from CHAMP and Ørsted data. The root mean square errors of our main field candidates, for the internal field to spherical harmonic degree 13, are estimated to be less than 8 nT at the Earth's surface. Our secular variation candidates are estimated to have root mean square uncertainties of 12 nT per year. A hind-cast analysis of the geomagnetic field for earlier epochs shows that our secular acceleration estimates from post-2000 satellite data are inconsistent with pre-2000 acceleration in the field. This could confirm earlier reports of a jerk around 2000.0, with a genuine change in the secular acceleration.

Key words: Geomagnetism, field modeling, reference field, secular variation.

1. Introduction

The geomagnetic field at the Earth's surface is strongly dominated by the long wavelength main field from the Earth's core. For numerous applications in navigation and ionospheric modelling the geomagnetic field is well approximated by this main field component. Furthermore, marine, aeromagnetic and ground magnetic surveys in geophysical exploration and geological mapping require the subtraction of a standard main field model. For these purposes, the International Association of Geomagnetism and Aeronomy (IAGA) publishes the International Geomagnetic Reference Field (IGRF), which includes a spherical harmonic (SH) representation of the main field (MF) in 5 year intervals, as well as the predicted secular variation (SV) for the coming 5 year period. The IGRF is compiled by a task force of IAGA working group V-MOD from submitted candidate models. The 10th generation IGRF candidate models were submitted in early October, 2004. Here, we describe the three candidate models for MF and three candidates for SV which were produced and submitted by the National Geophysical Data Center (NGDC) in collaboration with GeoForschungsZentrum (GFZ).

With the availability of more than five years of magnetic measurements from dedicated satellites (Ørsted, launched 1999 and CHAMP, launched 2000), combined with the long series of observatory measurements, the geomagnetic com-

munity currently has an excellent basis for deriving highly accurate main field models. Without damping, the static internal part of the field can now be derived to SH degree 77 (Maus *et al.*, 2005d), while the SV can be resolved to degree 13 and the acceleration to degree 10, as indicated in the power spectra of Fig. 1, below.

Here, we first describe our candidate models and input data selection procedures, roughly following the information requested by an informal checklist recommended by Frank Lowes (internal IAGA communication). Finally, we provide error estimates based on the comparison of independent CHAMP and Ørsted models and investigate our ability to forecast the magnetic field for the coming epoch by hind-casting the field for previous epochs.

2. Description of Candidate Models

Making use of the simultaneous availability of CHAMP and Ørsted vector data measurements, we have derived separate, independent CHAMP and Ørsted MF and SV candidate models, as well as a combined model. To improve long term stability, our combined model candidate for SV 2005–2010 also includes observatory annual means since 1995.5.

Our candidates for the main field in 2005 are:

- MF-1) A CHAMP-only model
- MF-2) An Ørsted-only model
- MF-3) A combined CHAMP and Ørsted model

Our candidates for the SV from 2005 to 2010 are:

- SV-1) A CHAMP-only model
- SV-2) An Ørsted-only model

Copyright © The Society of Geomagnetism and Earth, Planetary and Space Sciences (SGEPSS); The Seismological Society of Japan; The Volcanological Society of Japan; The Geodetic Society of Japan; The Japanese Society for Planetary Sciences; TERRAPUB.

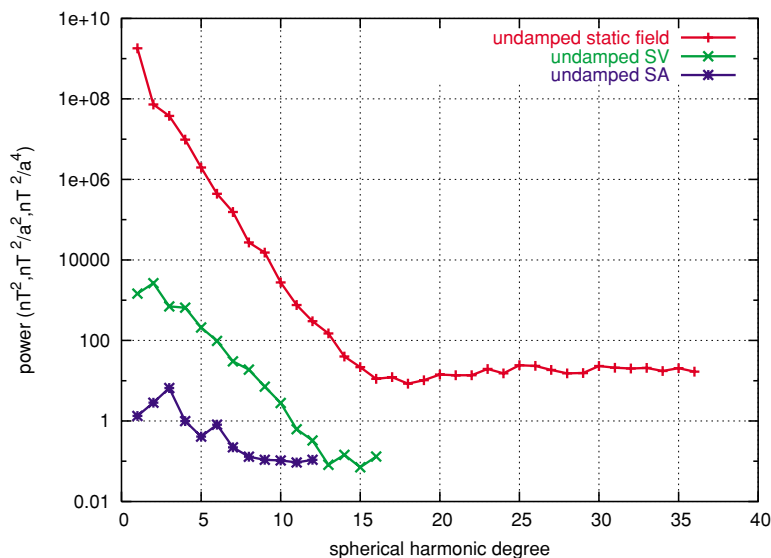


Fig. 1. Power spectra of undamped field models at the Earth's surface provide a good indication of noise levels in the data. The present noise floor in the data used for our CHAMP/Oersted parent model is at 0.1 (nT/a)^2 for the secular variation (SV) and at $0.1 \text{ (nT/a}^2\text{)}^2$ for the acceleration (SA), meaning that the SV has to be damped above degree 13 and the SA above degree 10. The static part of the field levels off at degree 16 due to the crustal magnetic field.

SV-3) A combined model from CHAMP, Ørsted and observatory annual means since 1995.0.

For all SV candidates the SV is extrapolated to 2007.5 by estimating 2nd time derivatives of the SH coefficients. These are also called quadratic secular variation or secular acceleration.

The coefficients are taken as subsets of higher degree models (parent models), with the static Gauss coefficients (g) to degree 36, secular variation (\dot{g}) to degree 16 and secular acceleration (\ddot{g}) to degree 12.

2.1 Input data

All parent models were derived from three independent data sets:

- 1) CHAMP data from Aug/00, scalar to Jul/04, vector to Apr/04
- 2) Ørsted scalar and vector data from Apr/99 to Jul/04
- 2a) Ørsted scalar and vector data from Jul/00 to Jul/04
- 3) First differences of observatory annual means for 1995 to 2003

Observatory annual means were taken from the NGDC Space Physics Interactive Data Resource (<http://spidr.ngdc.noaa.gov/spidr/index.jsp>). After plotting the residuals of annual mean differences against main field model POMME-2.1 and removing obvious outliers by visual inspection, the remaining data set has 933 annual mean differences from 187 observatories.

The data set 2a) was used to verify whether differences between Ørsted and CHAMP models were due to the different data sources or due to genuine differences in the secular acceleration of the field before and after 2000.

Table 1. The RMS of residuals for all available quiet night-time data (0–4 LT, $K_p < 2$, $Dst < 20$, CHAMP single and dual-head modes) of 2000–2004, against the model Ørsted-04i-04 (Olsen, 2004). This model is partly based on CHAMP scalar data, but not on CHAMP vector data. Note that RMS errors for Ørsted are lower for the field component pointing in the direction of the star camera bore sight.

	Ørsted RMS	CHAMP pre-cal RMS	CHAMP post-cal RMS
X	7.9	13.5	6.2
Y	7.0	9.9	5.0
Z	5.4	9.6	4.7
F	3.5	3.9	3.9

2.2 CHAMP Star Imager Calibration

An important step in pre-processing vector satellite magnetic measurements is the calibration of the alignment between the internal coordinate system of the vector magnetometer and the internal coordinate system of the star imager. Since these coordinate systems experience small (but significant) changes in their orientation against each other, a regularly updated calibration is essential. This calibration has been carried out for Magsat and Ørsted data, but not for the present CHAMP level-2 data. The final level-3 data will be fully corrected for this effect.

As a preliminary calibration we have estimated a continuous time series of the misalignment angles. A 3-day window was moved over the CHAMP vector data set. From the night-side data in the range of -60° to $+60^\circ$ latitude three misalignment correction angles were estimated by minimizing the root mean square (RMS) of the vector component residuals. The procedure is robust because constant misalignments have signatures that are distinctly different from those of genuine magnetic fields. Nevertheless, strong non-potential fields during magnetically disturbed times can

contaminate this calibration.

Once the time series of misalignment angles has been estimated, a simple point-by-point correction can be applied to all CHAMP vector data. The calibration file, a C-language procedure callable from FORTRAN, and a Matlab interface are available at <http://www.gfz-potsdam.de/pb2/pb23/SatMag/sca.html>.

Applying the correction significantly reduces the residuals of CHAMP vector data. Table 1 shows the RMS difference between data and a field model for pre- and post-calibrated data, and comparing these with the RMS of Ørsted data. Considering that higher residuals are expected for CHAMP data, due to its closer proximity to crustal and ionospheric sources (as manifested in F), the correction reduces CHAMP vector residuals to well below Ørsted levels. Thus, the correction realizes the potential of the low attitude noise of CHAMP's dual head star imager.

2.3 Correction for diamagnetic effect of ambient plasma

CHAMP satellite magnetic measurements are affected by the diamagnetic effect of the ambient plasma (Lühr *et al.*, 2003), which decreases magnetic field readings. The effect is of the order of a few nT and is strongest near the magnetic equator in the pre-midnight hours. Using the electron density and temperature readings from CHAMP's Planar Langmuir Probe, a simple diamagnetic correction was applied to the CHAMP data. This correction cannot be applied to Ørsted data due to the lack of electron density and temperature measurements. However, due to Ørsted's higher altitude, the plasma is thinner and the diamagnetic effect on the magnetic field is much smaller.

2.4 Correction for tidal ocean flow magnetic signal

Tidal movement of conducting seawater through the Earth's magnetic field induces electric fields, currents, and secondary magnetic fields, which reach about 7 nT at the ocean surface and 3 nT at satellite altitude. These fields are clearly visible in satellite data and closely coincide with independent predictions from tidal ocean flow models (Tyler *et al.*, 2003). The satellite measurements were corrected for the eight major tidal constituents, using the modelling method of Maus and Kuvshinov (2004).

2.5 Data selection and rejection procedures

Since our models do not include ionospheric contributions and only represent the portion of the magnetic field which dominates during undisturbed times, rigorous data selection criteria had to be applied. We follow the criteria of Olsen (2002) and include recent recommendations from Ritter *et al.* (2004). The following criteria were applied:

- 1) $Kp \leq 1+$, $Kp \leq 2$ for previous 3 h
- 2) $|Dst| < 30$ nT, $|d(Dst)/dt| < 3$ nT/h in previous 3 h
- 3) For polar latitudes: $|IMF-By| < 8$ nT
- 4) For polar latitudes: -2 nT $< IMF-Bz < 6$ nT
- 5) For mid latitudes: Vector data only up to 50 deg Mag Lat
- 6) For internal field: Sun at least 5 deg below horizon
- 7) For CHAMP mid latitude: $22:00 < \text{local time (LT)} < 5:00$

8) For Ørsted mid latitude: $21:00 < LT < 5:00$

9) All satellite data were checked for outliers against an initial field model (POMME-2.1)

10) Observatory annual means were plotted in terms of SV and noisy stations were eliminated

2.6 Parameterisation of external fields

During night time, the ionisation of the atmosphere is negligible at lower latitudes and ionospheric currents can be assumed negligible. At higher latitudes this is not valid, and additional data selection criteria have to be imposed (see criteria 3 and 4 under data selection). With such data selection, it is possible to exclude the ionosphere from the parameterisation of the parent field models.

The distant magnetosphere, on the other hand, has a continuous presence, even during quiet times. These external fields are largely sun-synchronous. Consequently, they are best described in Solar Magnetic (SM) and Geocentric Solar Magnetospheric (GSM) coordinates (Maus *et al.*, 2005a). Since it is not possible to estimate a sun-synchronous degree-2 external field from night side data alone, the external field was estimated from a combined CHAMP/Ørsted data set of the same period with full local time coverage. This magnetospheric field model was then subtracted from the night side data before estimating the internal field.

Our external field has 12 coefficients:

- 1) A coefficient for a uniform field aligned with the z-axis in SM for the steady ring current
- 2) A scaling factor for the Est/Ist dynamic ring current correction (Maus and Weidelt, 2004; Olsen *et al.*, 2005)
- 3) Eight coefficients for a stable degree-2 external field in GSM
- 4) Two coefficients accounting for IMF-By correlated fields (Lesur *et al.*, 2005), giving the correlation between IMF-By and uniform fields Y1,1 and Y1,-1 in GSM.

The GSM fields are coupled to the corresponding induced fields in the Earth-fixed frame, GEO, using the semi-global Earth conductivity model (model B) of Utada *et al.* (2003). Induced fields with multi-annual and multi-diurnal periods therefore did not have to be separately parameterised. Details of the parameterisation are described in Maus and Lühr (2005b).

The 12 magnetospheric field coefficients were determined from CHAMP and Ørsted scalar data at all latitudes and local times, with added CHAMP and Ørsted vector data at mid latitudes and all local times. The determined values are given in Table 2.

2.7 Extrapolation to epoch

For the main field in 2005.0, the Gauss coefficients, g , were obtained by expanding the model up to degree 13 as $g(t) = g + \dot{g}t + 0.5t^2\ddot{g}$, where $t = 0$ in 2002.5.

For the SV at 2007.5, the SV coefficients, \dot{g} , were predicted as $\dot{g}(t) = \dot{g} + t\ddot{g}$, where $t = 0$ in 2002.5.

2.8 Weights allocated to the different kinds of data

The individual data were weighted to achieve equal area weight over the sphere within each data set. The anisotropic

Table 2. Magnetospheric field model coefficients estimated from CHAMP and Ørsted satellite data with full local time coverage.

		Degree n	Order m				
			0	1	-1	2	-2
SM	Stable field	1	7.54				
	Est/Ist factor	1	(0.78)				
GSM	Stable field	1	13.15	0.20	0.02		
	Stable field	2	0.11	-0.11	1.31	-0.14	0.21
	IMF By penetration	1	0.12	-0.23			

Table 3. Weights given to the data sets for each model.

	CHAMP		Ørsted		Observatory annual mean differences
	Scalar	Vector	Scalar	Vector	Vector
Model	Global	50°...50°	Global	50°...50°	Global
MF-1	50%	50%			
MF-2			50%	50%	
MF-3	25%	25%	25%	25%	
SV-1	50%	50%			
SV-2			50%	50%	
SV-3	23%	23%	23%	23%	8%

covariance matrix for Ørsted was normalized to unity by dividing each coefficient by $\sqrt[3]{d}$, where d is the determinant of the covariance matrix. Furthermore, the sum of all weights within one data set was normalized to unity. The weights given to the individual data sets in each of the candidate models are summarized in Table 3.

2.9 Regularisation

Power spectra can be used to infer at which spherical harmonic degree noise begins to dominate over genuine signal. Figure 1 shows the Mauersberger/Lowes spectra of our combined CHAMP/Ørsted parent model MF-3. It indicates a noise threshold of about 0.1 nT², meaning that no damping is required for the static field, while the secular variation is resolved to degree 13 and the acceleration is resolved to degree 10.

Therefore, no regularisation was applied to the Gauss coefficients of the static part of the field. For the secular variation, degrees 14–16 of \dot{g} were damped by increasing the diagonals of the normal matrix to impose a decreasing spectrum of \dot{g} , and degrees 11–12 of \ddot{g} were damped accordingly to impose a decreasing spectrum of \ddot{g} .

2.10 Method used to solve the Least Squares equations

We used a direct solver, via eigenvectors and eigenvalues of the normal matrix $A^T A$. The anisotropic covariance, motivated by anisotropy in the angular determination by a single star camera, was initially used for Ørsted vector data, but was finally dropped because the anisotropic weighting was found to increase the difference between the separate CHAMP and Ørsted models. We believe that this may be due to the fact that Ørsted is not truly a rotating satellite. The attitude only changes by a couple of tens of degrees. Using anisotropic weights for a non-rotating satellite systematically down-weights certain directions. This may have a negative impact on the quality of the solution.

3. Model Verification and Estimates of Uncertainty

Here, we present two ways of assessing the reliability of the derived candidate models. The first is to directly compare the MF and SV coefficients of the two independent CHAMP and Ørsted models in order to obtain an estimate of the variance in the coefficients. The second is to hind-cast the known field for past epochs. Due to the temporal symmetry in the geomagnetic field, the ability to hind-cast the past field may provide a measure of the reliability of forecasts for the upcoming epoch.

3.1 Estimates of model uncertainty

With the simultaneous availability of CHAMP and Ørsted data, separate models have been estimated from both data sets. Indeed, the differences between each of the coefficients were provided as error estimates in the tables of submitted model coefficients. For the combined models, we supplied the RMS of the differences of the combined model to the individual Ørsted and CHAMP models as our error estimates. Table 4 lists the mean field difference [dB] over the surface of the Earth, as given by the square root of the sum of the Mauersberger/Lowes powers of the coefficient differences.

While we argue that these uncertainty estimates are likely to be fairly realistic, we point out, that the difference between independent models covers only the uncertainties associated with the input data. Not covered is the uncertainty of the model parameterisation itself. For example, a discontinuity in the 2nd time derivative of the field (a so-called jerk) could lead to significantly larger deviations of the true field from our models.

3.2 Verification of prediction uncertainties by hind-casting the field for previous epochs

Since there is no obvious reason why the geomagnetic field should behave differently for forward and backward directions in time, presumed model errors for the future can

Table 4. Mean vector field differences between independent CHAMP and Ørsted models at the Earth's surface. The models included quadratic terms referenced to $t = 0$ at 2002.5. The extrapolation to the dates given in the top row was done using the linear and quadratic terms.

CHAMP-Ørsted	2002.5	2005	2007.5	2010
Main field to degree 13	3.07 nT	7.51 nT	30.42 nT	70.01 nT
SV to degree 8	1.1 nT/a	5.9 nT/a	12.0 nT/a	18.2 nT/a

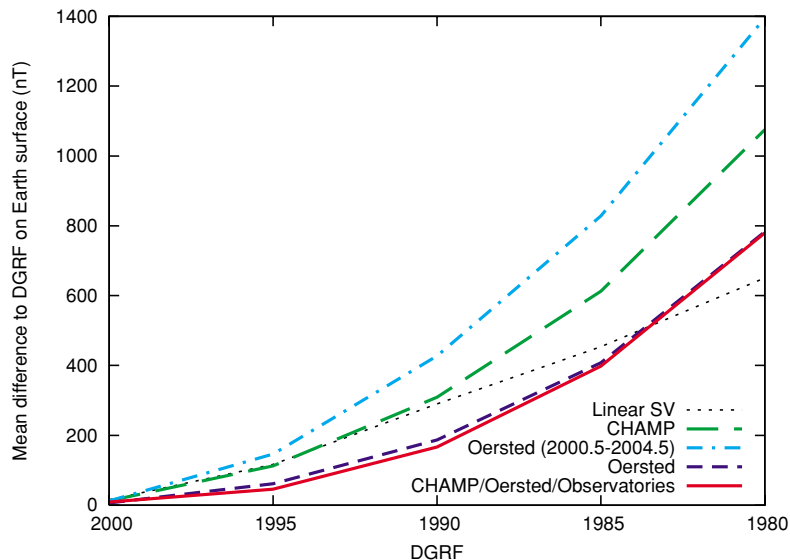


Fig. 2. Root mean square vector field difference over the Earth's surface between our parent models and previous DGRFs. A model's performance may be influenced by the data quality, length of the data period (stability), as well as by the proximity of the nearest measurement (2000.5 for CHAMP, 1999.2 for Ørsted, 1995.5 for the combined satellite, observatory model). The poor performance of the CHAMP (green) and comparable Ørsted (cyan) models may be due to a genuine change in the 2nd time derivatives of the field at around 2000.

be assessed by hind-casting the known field of the past. As for Table 4, this test cannot be performed using the submitted candidates themselves, but has to be carried out using the parent models which include the 2nd time derivatives of the coefficients.

Figure 2 shows the result for the CHAMP, Ørsted and the combined CHAMP/Ørsted/observatory parent models. In all cases, the 1st and 2nd time derivatives of these models are used to predict the main field for the previous times. The dashed line shows a backward extrapolation using only the linear secular variation in 2002.5, which is now known with very high accuracy. The hind cast analysis suggests that using the secular acceleration can improve the forecast of the field for periods of up to 15 years, if more than five years of data coverage are available.

As expected, the best hind-casting result is achieved by the model including observatory annual means back to 1995. In fact, we would have expected an even better result for this model. However, two effects are inseparably mixed here. The long time series of observatory data is expected to provide additional stability of the secular acceleration estimate. This should have a positive effect on the reliability of the SV candidate for the upcoming epoch. On the other hand, the data basis for the model included measurements back to 1995. The better hind-cast result may merely reflect the inclusion of this early data. For this model, past accuracy is therefore a poor indicator for future performance since a data set for the upcoming epoch, corresponding to

the early data, is obviously not available.

A surprising result is that the CHAMP-only model (green) fares significantly worse than the Ørsted model (dark blue). This contrasts with our experience that the CHAMP data, after the necessary attitude corrections, are cleaner and have a better coverage than the Ørsted data. There could be two reasons for this result: Either the CHAMP data have a systematic error, caused, for example, by attitude uncertainty or its low altitude orbit through regions of dense plasma. Alternatively, a jerk could have occurred around 2000.0, and a significant change in the 2nd time derivatives of the field would then compromise the ability of a post-2000 data set to hind-cast the pre-2000 field. Indeed, a possible jerk in 1999 was reported by Manda *et al.* (2000) and was confirmed by Sabaka *et al.* (2004). To investigate the impact of a change in the secular acceleration, we computed a new model using only Ørsted data after 2000.5 (cyan in Fig. 2). Interestingly, this model performs even worse in hind-casting the pre-2000 field. This supports the hypothesis that there has been a genuine change in the 2nd time derivatives of the geomagnetic field. This finding has been substantiated in the evaluation of candidate models (Maus *et al.*, 2005c).

4. Summary and Conclusions

The new satellite magnetic missions have enabled geomagnetists to derive main field models in unprecedented accuracy. Independent CHAMP and Ørsted models indicate a

root mean square error of our MF-2005 candidates of less than 8 nT at the Earth's surface. In contrast, the forecast of the secular variation is fraught with much larger uncertainties, estimated at 12 nT per year in 2007.5. This is partly caused by the chaotic behaviour of the field but may also be due to a lack in our understanding of the true field dynamics. It is expected that the ongoing satellite missions will enable us to get a better handle on predicting the field into the future.

An interesting question arises from a hind-cast analysis of the magnetic field. While quadratic terms (2nd time derivatives) appear to improve the hind cast of the magnetic field for periods back to 15 years, we find that the quadratic terms estimated from post-2000 CHAMP and Ørsted data lead to very poor hind cast results. Whether this is due to systematic errors in these models, or due to a genuine change in the secular acceleration is an interesting question to be answered in the near future.

Acknowledgments. The CHAMP mission and data center are operated by GeoForschungsZentrum Potsdam, Germany, supported by the German Aerospace Center (DLR) and by the Federal Ministry of Education and Research (BMBF). The Danish Meteorological Institute, supported by the Danish Space Research Institute and the Ministries of Trade, Research and Transport operates the Ørsted satellite mission and data center. The INTERMAGNET program provides valuable support and resources, which help the numerous unnamed individuals from many countries, private institutions, and government agencies around the world, that collect and process magnetic field data at geomagnetic observatories worldwide and kindly contributed data essential for the development of the WMM. In addition, observatory data and magnetic indices were provided by the World Data Centers in Copenhagen, Edinburgh, and Boulder.

References

- Lesur, V., S. Macmillan, and A. Thomson, A magnetic field model with daily variations of the magnetospheric field and its induced counterpart in 2001, *Geophys. J. Int.*, **160**, 79–88, 2005.
- Lühr, H., M. Rother, S. Maus, W. Mai, and D. Cooke, The diamagnetic effect of the equatorial Appleton anomaly: Its characteristics and impact on geomagnetic field modelling, *Geophys. Res. Lett.*, **30**, 1906, doi:10.1029/2003GL017407, 2003.
- Mandea, M., E. Bellanger, and J.-L. Le Mouél, A geomagnetic jerk for the end of the 20th century?, *Earth Planet. Sci. Lett.*, **183**, 369–373, 2000.
- Maus, S., H. Lühr, G. Balasis, M. Rother, and M. Mandea, Introducing POMME, the Potsdam Magnetic Model of the Earth, in *CHAMP Mission Results II*, pp. 293–298, Springer Berlin, 2005a.
- Maus, S. and H. Lühr, Signature of the quiet-time magnetospheric magnetic field and its electromagnetic induction in the rotating Earth, *Geophys. J. Int.*, 2005b (in press).
- Maus, S. and P. Weidelt, Separating the magnetospheric disturbance magnetic field into external and transient internal contributions using a 1D conductivity model of the Earth, *Geophys. Res. Lett.*, **31**, L12,614, 10.1029/2004GL020,232, 2004.
- Maus, S., S. Macmillan, F. Lowes, and T. Bondar, Evaluation of candidate geomagnetic field models for the 10th generation of IGRF, *Earth Planets Space*, **56**, this issue, 1173–1181, 2005c.
- Maus, S., M. Rother, K. Hemant, H. Luehr, C. Stolle, A. Kuvshinov, and N. Olsen, Earth's crustal magnetic field determined to spherical harmonic degree 90 from CHAMP satellite measurements, *Geophys. J. Int.*, 2005d (submitted).
- Maus, S. and A. Kuvshinov, Ocean tidal signals in observatory and satellite magnetic measurements, *Geophys. Res. Lett.*, **31**, L15313, 10.1029/2004GL020090, 2004.
- Olsen, N., A model of the geomagnetic field and its secular variation for epoch 2000 estimated from Ørsted data, *Geophys. J. Int.*, **149**, 454–462, 2002.
- Olsen, N., New parameterization of external and induced fields for geomagnetic field modeling, Geophysical Research Abstracts Volume 6, Abstracts of the Contributions of the EGU General Assembly, Nice, France, 2004.
- Olsen, N., T. J. Sabaka, and F. Lowes, New parameterization of external and induced fields in geomagnetic field modeling, and a candidate model for IGRF 2005, *Earth Planets Space*, **57**, this issue, 1141–1149, 2005.
- Ritter, P., H. Lühr, A. Viljanen, and S. Maus, High-latitude ionospheric currents during very quiet times: their characteristics and predictability, *Annales Geophysicae*, **22**, 2001–2014, 2004.
- Sabaka, T., N. Olsen, and M. E. Purucker, Extending comprehensive models of the Earth's magnetic field with Ørsted and CHAMP data, *Geophys. J. Int.*, **159**, 521–547, 2004.
- Tyler, R., S. Maus, and H. Lühr, Satellite observations of magnetic fields due to ocean tidal flow, *Science*, **299**, 239–241, 2003.
- Utada, H., H. Koyama, H. Shimizu, and A. D. Chave, A semi-global reference model for electrical conductivity in the mid-mantle beneath the north Pacific region, *Geophys. Res. Lett.*, **30**, 10.1029/2002GL016092, 2003.

S. Maus (e-mail: Stefan.Maus@noaa.gov), S. McLean, D. Dater, H. Lühr, M. Rother, W. Mai, and S. Choi